Journal of Zhejiang University-SCIENCE A (Applied Physics & Engineering)
ISSN 1673-565X (Print); ISSN 1862-1775 (Online)
www.jzus.zju.edu.cn; www.springerlink.com
E-mail: jzus@zju.edu.cn

In-situ characterization of gas-liquid precipitation reaction in a spray using rainbow refractometry*

Xue-cheng WU[1], Can LI[1], Jian-zheng CAO[1], Yong-xin ZHANG[1],
Ling-hong CHEN†‡[1], Gerard GRÉHAN[2], Ke-fa CEN[1]

[1]*State Key Laboratory of Clean Energy Utilization, Zhejiang University, Hangzhou 310027, China*
[2]*UMR 6614/CORIA, Normandie University, CNRS, bp12 76801 Saint Etienne du Rouvray, France*
†E-mail: chenlh@zju.edu.cn

Received May 5, 2017; Revision accepted July 24, 2017; Crosschecked Dec. 15, 2017

Abstract: Gas-liquid precipitation reactions in terms of a spray exist widely in energy, chemical, and environmental engineering. In this paper, a rainbow refractometry-based method is used to measure the reaction process of these spray-based gas-liquid precipitation reactions in a non-intrusive way. Rainbow refractometry can simultaneously provide information on thermochemical and physical properties of droplets. A global rainbow measurement system was built to characterize a CO_2 absorption reaction. Rainbow signals of spray droplets of $Ca(OH)_2$ solutions before and after CO_2 absorption were recorded and processed. Results indicated that the average refractive index of saturated H_2O-$Ca(OH)_2$ solution was 1.335 69, which accorded with the Abbe measurement. After the absorption reaction, the refractive index of droplets decreased to 1.335 17 which is close to that of water. The reaction extent was therefore reflected in the change of the refractive index of droplets. An extra experiment of CO_2 absorbed by $Ba(OH)_2$ solutions was conducted. The refractive index of droplets decreased with the reaction process, which acted well as an evolution indicator of the reaction. A heat transfer analysis of the reaction was also carried out. Due to the high heat dissipation performance of fine droplets, the temperature increase in the measurement volume was estimated to be less than 0.61 K, which has almost no effect on the measured results. The rainbow refractometry-based method shows good potential for in-situ characterization of a gas-liquid precipitation reaction.

Key words: Rainbow refractometry; In-situ characterization; Refractive index; Gas-liquid precipitation reaction
https://doi.org/10.1631/jzus.A1700240 **CLC number:** TK31

1 Introduction

Environmental issues, such as haze weather and global warming, are becoming a major concern for the public. Excessive SO_x and NO_x, mainly produced by the burning of fossil fuels, are two causes of haze formation. Nontoxic CO_2 is the major source of greenhouse gases (GHG) believed to cause global warming and represents 76.7% of GHG. Recently, China committed to promoting the ultra-low emissions of coal-fired power plants. Wet flue gas desulfurization (WFGD) (Gao et al., 2008, 2009) and CO_2 capture by monoethanolamine are two ways of pollutant and emission control, which all involve the gas-liquid absorption reaction. WFGD has been used as a leading technology for many years in the field of wet desulfurization and denitrification in a power plant. The slurry droplets of lime used as the desulfurization or denitrifying agent have a chemical

‡ Corresponding author
* Project supported by the National Natural Science Foundation of China (No. 51576177), the Major Program of the National Natural Science Foundation of China (No. 51390491), the National Basic Research Program of China (No. 2015CB251501), and the Program of Introducing Talents of Discipline to University (No. B08026), China
ORCID: Xue-cheng WU, https://orcid.org/0000-0001-9897-8776

absorption precipitation reaction with SO_2 or NO_x during the atomization. They ultimately appear in the form of droplets with solid inclusion in the air. Therefore, in-situ characterization of the evolution of the gas-liquid absorption precipitation reaction is beneficial for monitoring and improving the removal efficiency of pollutants.

So far, few studies have focused on the in-situ characterization of the gas-liquid absorption precipitation reaction. As an advanced optical diagnostic method, rainbow refractometry is a potential technique for the measurement of refractive index (RI) and size distribution of spray droplets by recording and analyzing the elastic scattering light around the rainbow angle in real time. The standard rainbow technique (SRT) for measuring a single droplet or identical droplets was first proposed by Roth et al. (1990). In order to overcome the problems of ripple structures and non-spherical droplets, van Beeck et al. (1999) invented a global rainbow technique (GRT) for measuring the mean RI and size distribution of polydispersed droplets by extending the exposure time and enlarging the aperture. Wu et al. (2014) presented a 1D rainbow refractometry which simultaneously obtains parameters of droplets on a line, and rainbow refractometry was extended to a 1D measurement technique. Rainbow refractometry (Wu et al., 2017) has achieved great popularity in measuring concentration (Zhao and Qiu, 2006; Wilms and Weigand, 2007; Wu et al., 2012), non-sphericity (van Beeck and Riethmuller, 1996; Lohner et al., 1999; Saengkaew et al., 2009; Yu et al., 2013a, 2013b), RI gradient (Saengkaew et al., 2007; Rosebrock et al., 2016; Song et al., 2016; Li et al., 2017), droplet diameter variations at the nanoscale as well as recently in the diagnostic of spray evaporation (Promvongsa et al., 2017) or combustion (Letty et al., 2013; Verdier et al., 2016) and pollutant removal (Ouboukhlik et al., 2015a, 2015b).

This paper investigates the in-situ characterization of the gas-liquid absorption precipitation reaction using rainbow refractometry for the first time. In this study, the measurement theories, including the principle of rainbow refractometry and parameter inversion, are introduced first, followed by the presentation of the experimental setup. Then, the signal processing and heat transfer are provided.

2 Measurement theories

2.1 Principle of rainbow refractometry

The path of light reflected and refracted at the equatorial plane of a droplet is shown in Fig. 1, where P is the Debye series, D is the droplet diameter, and α_r is the refractive angle. From geometrical optics and Snell's law, the scattering angle is given by

$$\theta=\pi+2\alpha-4\arcsin\left(\frac{\sin\alpha}{m}\right), \tag{1}$$

where θ denotes the scattering angle, α denotes the incident angle, and m denotes the relative RI of liquid to air. According to Eq. (1), a minimum named the geometrical rainbow angle exists at a specific incident angle. The geometrical rainbow angle θ_{rg} is expressed as

$$\theta_{rg}=2\arccos\left[\frac{1}{m^2}\left(\frac{4-m^2}{3}\right)^{3/2}\right]. \tag{2}$$

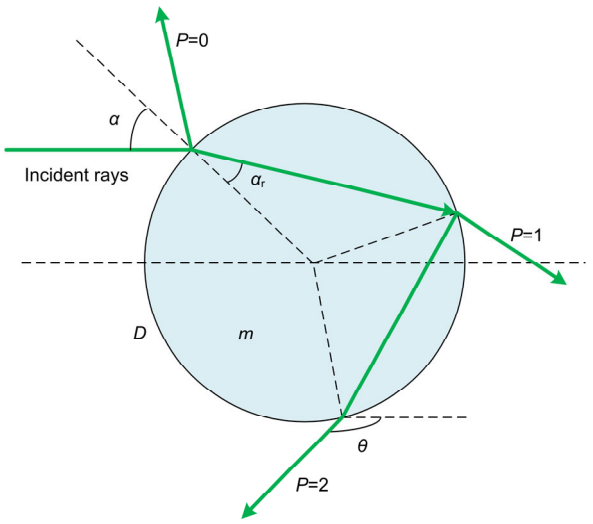

Fig. 1 Path of light reflected and refracted at the equatorial plane of a droplet

The geometrical rainbow angle θ_{rg} from Eq. (2) significantly depends on the RI of liquid (m). Although there are some deviations, the RI can be obtained from the angular location of the rainbow. The change in droplet size leads to a variation in angular spacing of the rainbow fringes. Thus, the

physical and thermochemical parameters of droplets can be determined from the intensity distribution of the rainbow.

2.2 Parameter inversion

The global rainbow signal of spray droplets is processed by the independent inversion algorithm proposed by Saengkaew (2005). The RI and size distribution are obtained by solving the equation using the non-negative least-squares algorithm:

$$I_{\mathrm{g}}=\begin{bmatrix} I_{\mathrm{g}}(\theta_1)\\ I_{\mathrm{g}}(\theta_2)\\ \vdots\\ I_{\mathrm{g}}(\theta_j)\end{bmatrix} =\begin{bmatrix} I(d_1,\theta_1,m), I(d_2,\theta_1,m),\cdots, I(d_i,\theta_1,m)\\ I(d_1,\theta_2,m), I(d_2,\theta_2,m),\cdots, I(d_i,\theta_2,m)\\ \vdots\\ I(d_1,\theta_j,m), I(d_2,\theta_j,m),\cdots, I(d_i,\theta_j,m)\end{bmatrix} \cdot\begin{bmatrix} N(d_1)\\ N(d_2)\\ \vdots\\ N(d_i)\end{bmatrix}=\boldsymbol{T}\cdot\boldsymbol{N}, \tag{3}$$

where $I_{\mathrm{g}}(\theta_j)$ is the total light intensity of the global rainbow at the scattering angle θ_j; $I(d_i, \theta_j, m)$ is the rainbow light intensity at the scattering angle θ_j for a droplet with an RI of m and diameter of d_i, which forms the rainbow coefficient matrix $\boldsymbol{T}$; $N(d_i)$ is the number of droplets with diameter d_i, and this forms the size distribution $\boldsymbol{N}$.

The light intensity-angle distribution of global rainbow I_{g} is recorded by an array CCD camera. Initial RI and size distribution are obtained from an initial estimation by solving the equation using the non-negative least-squares algorithm. The RI m and size distribution $\boldsymbol{N}$ are optimized by iteratively searching for the minimum absolute error of the recorded rainbow signal and the fitted rainbow signal using Brent's method. The fitted rainbow signal is computed using the modified Nussenzveig theory with correction coefficients (Saengkaew et al., 2006). This theory takes into account the interference between the light experiencing one internal reflection (P=2) and the ripple structure (external reflected light (P=0) interference with one internal refracted light). Eq. (4) (Nussenzveig, 1969) indicates the theorical calculations of the one internal refracted light around the rainbow angle.

$$\begin{aligned} f_{\mathrm{rainbow}}(x,\theta)=&-\frac{D}{2}\cdot\frac{16\exp\left(-\frac{\mathrm{i}\pi}{4}\right)}{27\sqrt{3}}\cdot\sqrt{\frac{\pi}{\sin\theta}}\\ &\cdot c\cdot(6sx)^{\frac{1}{6}}\cdot\exp\left(6\mathrm{i}cx+\mathrm{i}s\varepsilon x+\mathrm{i}A\varepsilon^2x+O\left(x\varepsilon^2\right)\right)\\ &\cdot\left\{A_{\mathrm{i}}\left[1+O(\varepsilon)+O\left(x^{-1}\right)\right]\left[\frac{(2x)^{2/3}c\varepsilon}{(3s)^{1/3}}\left(1+B\varepsilon+O\left(\varepsilon^2\right)\right)\right]\right.\\ &\left.+\frac{\mathrm{i}CA_{\mathrm{i}}'}{(2x)^{1/3}}\left[-\frac{(2x)^{2/3}c\varepsilon}{(3s)^{1/3}}\cdot\left(1+B\varepsilon+O\left(x\varepsilon^2\right)\right)\right]\right\}, \end{aligned} \tag{4}$$

where $x=\pi D/\lambda$ is the dimensionless size parameter, λ is the wavelength, $\varepsilon=\theta-\theta_{\mathrm{rg}}$ is the relative scattering angle, f_{rainbow} is the rainbow amplitude, O is infinitesimal asymptotic, A_{i} is the Airy function, A_{i}' is the derivative of A_{i}, and A, B, C, c, and s are the coefficients which only depend on the RI.

3 Experimental set up

An in-situ global rainbow experimental measurement system was built to characterize the evolution of the absorption of CO_2 by the H_2O-$Ca(OH)_2$ solution, and the schematic is shown in Fig. 2. A CO_2 jet was arranged in a vessel made of Plexiglas with a saturated H_2O-$Ca(OH)_2$ solution spray above the vessel. The measurement objects were spray droplets of a saturated H_2O-$Ca(OH)_2$ solution before the absorption reaction, and droplets of a H_2O-$CaCO_3$ suspension after the absorption. The experimental system comprised a spray generating system and an optical system.

The spray was generated by an ultrasonic nozzle (model YPWH32020L, frequency 20 kHz). A pump provided the necessary pressure (101–1010 kPa) for the transport of the measured liquid from the sample pool. The nozzle was placed on the top of the vessel, and created a spray with a mean droplet diameter of 60 μm and a mean velocity of about 1.2 m/s (for a

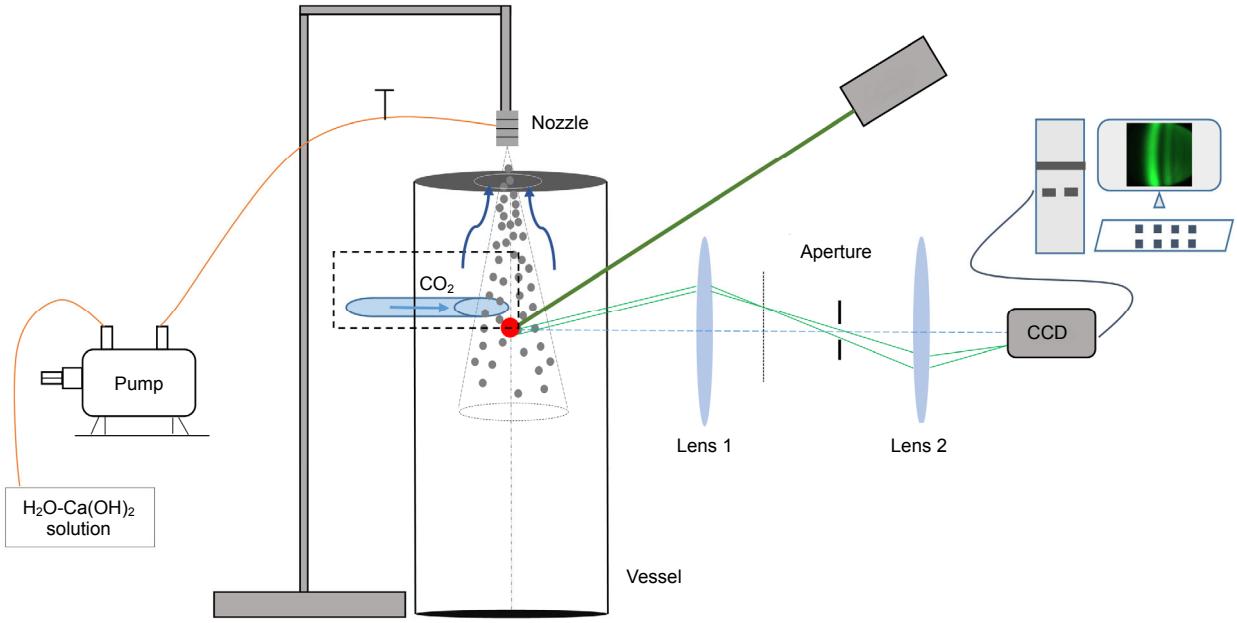

Fig. 2 Schematic of global rainbow experimental measurement system for characterization of CO_2 absorption reaction

pump flow rate of 180 ml/min). The measurement volume was located at the spray center, about 40 cm from the nozzle orifice. The CO_2 gas inlet, with a flow rate of 90 ml/min, was located around the measurement volume. This brought the gas and liquid into counter current exchange.

The optical system consisted of an optical platform, a single longitudinal mode laser (power=200 mW, λ=532 nm) with coherence length of 50 m, a CCD camera (resolution 2048×2048 pixels, pixel size: 7.4 μm/pixel), two plano-convex lenses (diameter=10 cm, focal length f=16 cm), an aperture, and a computer used to record and process the rainbow signals. The measurement volume was illuminated by a vertical polarized laser beam with a polarization ratio of 100. Scattering light around the rainbow angle of the droplets (P=2, about 132°–147°) was collected by the first lens. Located in the image plane of the measurement volume in lens 1, the aperture could effectively eliminate stray environmental light and control the measurement volume. The second lens conjugated the back focal plane of the first lens on the CCD. The scattering light at each scattering angle was recorded by different columns in the CCD. The two spherical lenses and one aperture, together with the CCD, form the global rainbow imaging system. The working distance (namely, distance from the measurement volume to lens 1) was 24 cm, and the aperture size was about 2 mm. The exposure time of the CCD camera with a tunable range of 20 μs–100 ms was fixed at 50 ms to record numerous superimposed rainbows on each frame. In addition, the relationship of scattering angle with CCD pixel was calibrated using a linear fitting method by a reflector mirror with a rotating accuracy 0.033°.

4 Results and discussion

4.1 Rainbow signals process and analysis

The RI of $Ca(OH)_2$ solutions at different mass fractions was measured by an Abbe refractometer (model 2WAJ) as a standard. Since the solubility of $Ca(OH)_2$ in 100 ml water is about 0.16 g at room temperature, $Ca(OH)_2$ solutions with mass fractions of 0%, 0.08%, and 0.16% were prepared using deionized water and $Ca(OH)_2$ powder and a microbalance. The room temperature, which also affected the RI, was about 24.2 °C measured by a K-type thermocouple.

It must be noted that the wavelength used in the Abbe refractometer was 589.3 nm which differed from 532 nm used in this experiment. Therefore, it is necessary to convert the results from 589.3 nm to 532 nm. The equation for the water RI as a function of wavelength and temperature has already been fully

studied, as given by Eq. (5) (Quan and Fry, 1995), and the converted results are also shown in Fig. 3. The deviation of RI introduced by the wavelength difference is equal to 2.0×10^{-3} under a temperature from 0 °C to 20 °C, illustrated in Fig. 3. The RI is significantly proportional to the mass fraction. The RI of the saturated H_2O-$Ca(OH)_2$ solution is about 1.3356, while that of water is about 1.3352. This preliminary experiment illustrated that there was obviously a corresponding relationship between the concentration of $Ca(OH)_2$ solutions and the RI.

$$\begin{aligned} n_T^{\lambda} &= 1.31405 - 2.02\times10^{-6}T^2 \\ &\quad + (15.868 - 0.00423T)\lambda^{-1} \\ &\quad - 4382\lambda^{-2} + 1.1455\times10^{6}\lambda^{-3}, \\ n_T^{532} &- n_T^{589.3} \\ &= (20.46106762 - 7.731200136\times10^{-3}T)\times10^{-4} \\ &\approx 2\times10^{-3}, \end{aligned} \tag{5}$$

where T denotes the temperature, and n_T is the RI at temperature T.

As shown in Fig. 4a, the global rainbow signals of the atomized droplets before and after CO_2 absorption were recorded, and the products were sampled and analyzed using an off-line microscope. It could be seen from the micrograph that lots of small $CaCO_3$ solid particles of size 1–3 μm appear after the absorption reaction. The number concentration of $CaCO_3$ particles with a mean size of 2 μm is around 23 in a droplet. The intensity curves of the rainbow signals before and after CO_2 absorption are shown in Fig. 4b. The absorption of CO_2 brings about a significant leftward shift in the increase part of the main peak. Due to the reduction of droplet diameter (about 8 μm), there exists a larger peak width for the rainbow signal after the reaction. The results of GRT indicate that the average RI of saturated H_2O-$Ca(OH)_2$ solution is 1.335 69 (λ=532 nm), which is consistent with Fig. 3. After absorption, the $Ca(OH)_2$ dissolved in the water is converted into insoluble $CaCO_3$ particles, and the average RI of the droplets decreases to 1.335 17, which is close to that of the deionized water calculated by Eq. (5). The measured RI for each condition was averaged from 30 rainbow signals, and the error bars were about 1.0×10^{-4}.

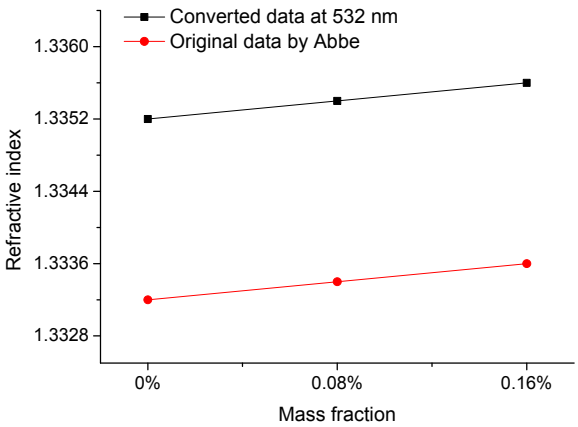

Fig. 3 Refractive index of $Ca(OH)_2$ solutions at different mass fractions

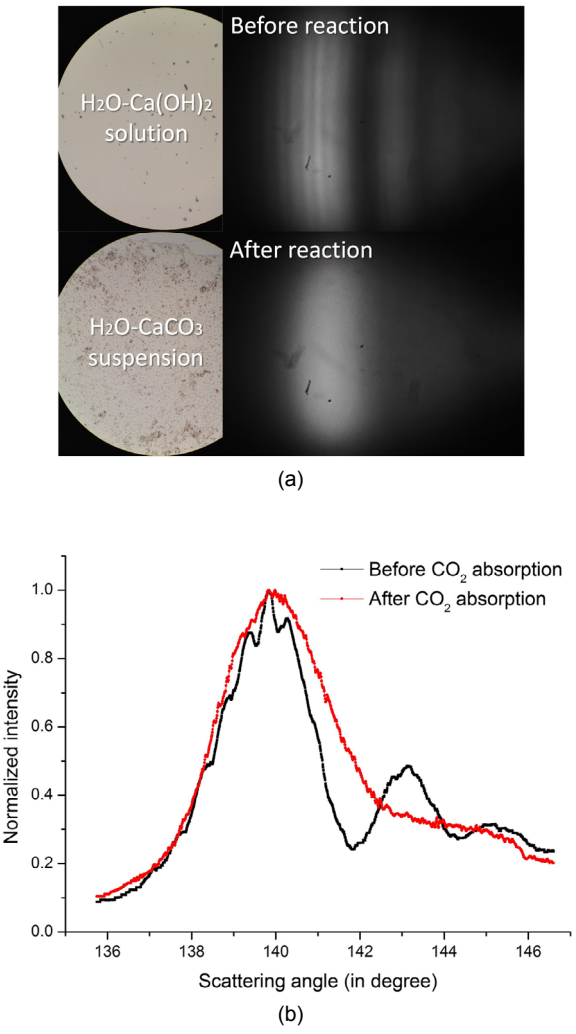

Fig. 4 Rainbow signals for H_2O-$Ca(OH)_2$ solution before and after CO_2 absorption (a) and intensity curves of the rainbow signals (b)

The chemical equation between $Ca(OH)_2$ and CO_2 is shown in Eq. (6). With the process of reaction, the concentration of $Ca(OH)_2$ falls with an increase in that of $CaCO_3$, while the total molarity is fixed. Based on the conclusions of our previous work, the solid inclusions (≤4 μm) at low concentrations have no effect on the measurement of the liquid RI. Small $CaCO_3$ solid particles as inclusions in the host droplet will obstruct some scattering rays, causing some disturbances on the primary and supernumerary bow. These disturbances to the rainbow pattern depend on the position, particle size, and number concentration of the inclusions. In the case of recording multiple droplets with inclusions at low concentration using GRT, the disturbances would be superimposed like the ripple structure and not affect the parametric measurement of the liquid phase. As illustrated in Fig. 5, the RI variances caused by different mass concentrations (C_m<6.92%) are about 2.0×10^{-4}. The RI of droplets decreases with the reaction process, and the amount of the reaction could be reflected in the shift of the rainbow angular location (i.e. RI of droplets). Therefore, the process of the precipitation reaction can be observed and analyzed by the in-situ measurement of GRT.

$$\mathrm{Ca(OH)_2(l)+CO_2(g)\rightarrow CaCO_3(s)+H_2O(l)}. \quad (6)$$

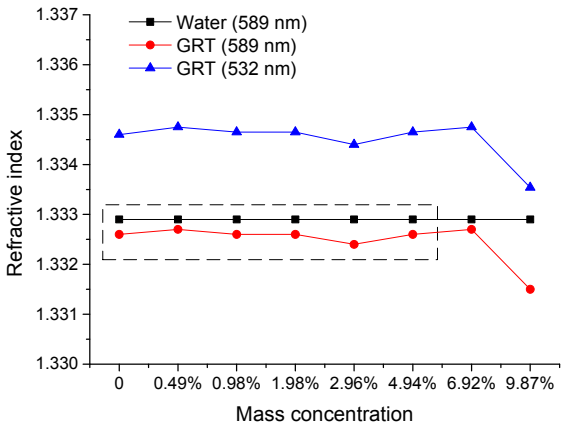

Fig. 5 Refractive index of droplets of H_2O-$CaCO_3$ suspensions (C_m=0%–9.87%) using GRT

The reaction rate, which is critical to the reaction, is limited by the concentration of reactants and mass transfer efficiency of diffusion and absorption. Traditional experimental study of the reaction rate is of that in the reactor. A certain concentration of H_2O-$Ca(OH)_2$ solution contained in a vessel reacts with CO_2 gas from pressure cylinders. The stirrer at the bottom of the reactor continuously stirs at a constant rate to speed up the reaction. The average reaction rate for saturated H_2O-$Ca(OH)_2$ solution in the literature is about 0.07 g/s (Haghnegahdar et al., 2011). Since the atomized droplet provides a larger surface area for contacting the reactants, heat transfer, mass transfer, and the chemical reaction occur simultaneously. When the liquid reacts with CO_2 in the form of atomized droplets, the reaction speed can be greatly increased, and the absorption efficiency can be improved. In this experiment, the liquid flow rate was 3 ml/s, and the solubility of $Ca(OH)_2$ at room temperature is 0.00166 g/ml. The reaction between injected spray droplets and CO_2 takes less than 71.1 ms which is short enough to be assumed as an instantaneous process. Therefore, the concentration gradient of the reactant in the measurement volume can be ignored.

$Ba(OH)_2$ solutions were also selected to absorb CO_2, due to their greater solubility (27 times more than that of $Ca(OH)_2$). CO_2 at different flow rates (0, 2, 4, 6, 8, 10, and 12 ml/s) was pumped to react with $Ba(OH)_2$ solutions (C_m=3.0%), and these represent different reaction processes. The rainbow signals and the micrographs at the seven working conditions were recorded and processed, as shown in Fig. 6. Because of the scattering extinction introduced by an increasing number of generated solid particles, absolute light intensities of rainbow signals become smaller with the reaction process.

The off-line micrographs show that the small solid particles increase with the reaction process. In addition, RI has a one-to-one relationship with the micro-morphology of droplets, which in-situ reveals the reaction process. With the decrease of RI, the concentration of solid particles increases, which fits well with the results of the Abbe refractometer.

4.2 Heat transfer analysis

According to the position of the measurement volume and the velocity of the droplets, the contact time Δt is about 333 ms. During this time, there is in total $m_w=1.0\times10^{-3}$ kg $Ca(OH)_2$ (aq) (C_m=0.16%) injected from the nozzle, which is selected as the study object. The molecular weight of Calcium hydroxide is

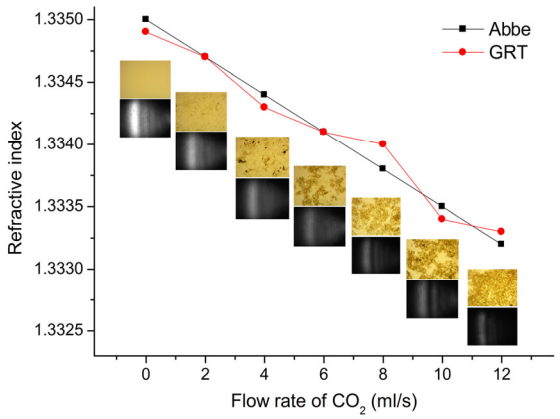

Fig. 6 Rainbow characterization of CO_2 absorption reaction in different processes (Abbe means the RI measured by Abbe refractometer)

74 g/mol. The chemical reaction enthalpy of Eq. (6) is about ΔH=−97.3 kJ/mol (298.15 K) (Zumdahl, 2009), and thus the heat release Q_r of the reaction is 2.1 J. The specific heat capacity of the aqueous solution is approximately equal to that of water, C_V=4.2 kJ/(kg·K).

The heat transfer between a droplet in the falling state and air could be classified as forced convection heat transfer for flow in a single sphere, and the coefficient h is calculated by the following equations:

$$Nu = 2 + \left(0.4Re^{1/2} + 0.06Re^{2/3}\right) Pr^{0.4} \left(\frac{\eta_\infty}{\eta_w}\right)^{1/4}, \quad (7)$$

$$Re = \frac{VD}{\nu}, \quad (8)$$

$$h = Nu \cdot \frac{\lambda_c}{D}, \quad (9)$$

where Nu denotes the Nusselt number, Re denotes the Reynolds number, Pr denotes the Prandtl number of air (Pr=0.708 56), η_∞ is the kinetic viscosity coefficient of air at room temperature (η_∞=1.821 48×10^{-5} kg/(m·s)), η_w is that at the droplet temperature (η_w=1.8462×10^{-5} kg/(m·s)). The qualitative temperature is room temperature (T_∞=298.15 K), and characteristic length is the droplet diameter (D=60 μm). In addition, Eq. (7) (Whitaker, 1972) is valid in two ways: 0.71<Pr<380, and 3.5<Re<76 000. In Eq. (8), V is the air velocity (V=1.2 m/s), and ν is the kinematic viscosity coefficient of air (ν=1.5617×10^{-5} m^2/s). In Eq. (9), λ_c is the thermal conductivity of air (λ_c= 0.025 854 W/(m·K)).

Based on the above formulas and input parameters, Re=4.61, Nu=2.89, and thus h=1245 W/(m^2·K).

The heat transfer equation is expressed as:

$$Q_r - Q_d = C_V m_w \Delta T, \quad (10)$$

$$Q_d = h \cdot A_s \cdot \overline{\Delta T} \cdot \Delta t, \quad (11)$$

$$A_s = N \cdot 4\pi d^2 = \frac{m_w}{\rho \frac{4}{3}\pi d^3} \cdot 4\pi d^2 = \frac{3m_w}{\rho d}, \quad (12)$$

$$\Delta T < \frac{Q_r}{\left(C_V m_w + h\frac{3m_w}{\rho d}\Delta t\right)}, \quad (13)$$

where Q_d is the heat dissipation, A_s is the total liquid superficial area, ρ is the aqueous density (ρ= 1000 kg/m^3), d is the droplet radius (d=30 μm), N is the droplet number of the study object, ΔT=$T_{droplet}$−T_∞ is the temperature difference between the droplets and the test environment, and $\overline{\Delta T}$ is the time mean temperature difference (absolutely $\overline{\Delta T} > \Delta T$). On the basis of the above equations and parameters, ΔT is estimated to be less than 0.05 K.

Considering the convection heat transfer between the droplets and the test environment, the temperature increase is less than 0.05 K. The heat transfer of reaction between $Ba(OH)_2$ solutions and CO_2 can be analyzed in the same way, with a maximum ΔT of less than 0.61 K.

The reaction heat, which depends on the concentration of the measured aqueous droplets, will lead to a ΔT, influencing the RI indirectly. From careful estimation, ΔT from the first reaction is less than 0.05 K, and ΔT from the second reaction is less than 0.61 K. In this case, the maximum RI variation for water is less than 6.0×10^{-5} which is within the measurement accuracy of rainbow refractometry. Therefore, the effect from the temperature increase on the results can be ignored, and the same applies to the temperature gradient.

5 Conclusions

Rainbow refractometry was used to measure the reaction process of a gas-liquid absorption precipitation reaction. Measurement theories, including the

principle of rainbow refractometry and parameters inversion, were introduced. A global rainbow experimental measurement system was built for in-situ characterization of the CO_2 absorption reaction. A preliminary experiment illustrated the feasibility of characterization of the concentration of $Ca(OH)_2$ solutions by refractive index. The rainbow signals of spray droplets of $Ca(OH)_2$ solution before and after CO_2 absorption were recorded and processed. The results of GRT indicated that the average refractive index of saturated H_2O-$Ca(OH)_2$ solution was 1.335 69, which accorded with Abbe measurement. After the reaction, the refractive index of droplets decreased to 1.335 17 which was close to that of water. The reaction extent was reflected in the shift of the rainbow angular location (i.e. refractive index of droplets). Pumping different flow rates of CO_2, an extra experiment on CO_2 absorbed by $Ba(OH)_2$ solution at different processes was conducted. The refractive index decreased as the reaction proceeded, which acted well as an evolution indicator of the reaction. The heat transfer of the absorption reaction was also analyzed based on a flow in single sphere model. After careful analysis, the temperature increase in the measurement volume was estimated to be less than 0.61 K, which was within the measurement accuracy of rainbow refractometry and could be ignored.

The feasibility of the preliminary investigation had been verified. All these results provide a new insight on the in-situ measurement of the gas-liquid precipitation reaction. The next step in our research will be to investigate the reaction rate and mass transfer for further control and optimization.

References

Gao X, Huo W, Luo, ZY, et al., 2008. CFD simulation with enhancement factor of sulfur dioxide absorption in the spray scrubber. *Journal of Zhejiang University-SCIENCE A*, 9(11):1601-1613. https://doi.org/10.1631/jzus.A0820507

Gao X, Guo RT, Ding HL, et al., 2009. Absorption of NO_2 into Na_2S solution in a stirred tank reactor. *Journal of Zhejiang University-SCIENCE A*, 10(3):434-438. https://doi.org/10.1631/jzus.A0820657

Haghnegahdar MR, Rahimi A, Hatamipour MS, 2011. A rate equation for $Ca(OH)_2$ and CO_2 reaction in a spouted bed reactor at low gas concentrations. *Chemical Engineering Research and Design*, 89(6):616-620. https://doi.org/10.1016/j.cherd.2010.10.019

Letty C, Renou B, Reveillon J, et al., 2013. Experimental study of droplet temperature in a two-phase heptane/air V-flame. *Combustion and Flame*, 160(9):1803-1811. https://doi.org/10.1016/j.combustflame.2013.03.017

Li H, Rosebrock CD, Wriedt T, et al., 2017. The effect of initial diameter on rainbow positions and temperature distributions of burning single-component n-alkane droplets. *Journal of Quantitative Spectroscopy and Radiative Transfer*, 195:164-175. https://doi.org/10.1016/j.jqsrt.2017.01.004

Lohner H, Lehmann P, Bauckhage K, 1999. Detection based on rainbow refractometry of droplet sphericity in liquid–liquid systems. *Applied Optics*, 38(7):1127-1132. https://doi.org/10.1364/AO.38.001127

Nussenzveig H, 1969. High-frequency scattering by a transparent sphere. II. Theory of the rainbow and the glory. *Journal of Mathematical Physics*, 10(1):125-176. https://doi.org/10.1063/1.1664747

Ouboukhlik M, Saengkaew S, Fournier-Salaün MC, et al., 2015a. Local measurement of mass transfer in a reactive spray for CO_2 capture. *The Canadian Journal of Chemical Engineering*, 93(2):419-426. https://doi.org/10.1002/cjce.22123

Ouboukhlik M, Godard G, Saengkaew S, et al., 2015b. Mass transfer evolution in a reactive spray during carbon dioxide capture. *Chemical Engineering & Technology*, 38(7):1154-1164. https://doi.org/10.1002/ceat.201400651

Promvongsa J, Vallikul P, Fungtammasan B, et al., 2017. Multicomponent fuel droplet evaporation using 1D global rainbow technique. *Proceedings of the Combustion Institute*, 36(2):2401-2408. https://doi.org/10.1016/j.proci.2016.08.010

Quan X, Fry ES, 1995. Empirical equation for the index of refraction of seawater. *Applied Optics*, 34(18):3477-3480. https://doi.org/10.1364/AO.34.003477

Rosebrock CD, Shirinzadeh S, Soeken M, et al., 2016. Time-resolved detection of diffusion limited temperature gradients inside single isolated burning droplets using rainbow refractometry. *Combustion and Flame*, 168:255-269. https://doi.org/10.1016/j.combustflame.2016.03.007

Roth N, Anders K, Frohn A, 1990. Simultaneous measurement of temperature and size of droplets in the micrometer range. *Journal of Laser Applications*, 2(1):37-42. https://doi.org/10.2351/1.4745251

Saengkaew S, 2005. Study of Spray Heat Up: on the Development of Global Rainbow Techniques. PhD Thesis, Rouen University, Rouen, France.

Saengkaew S, Charinpanitkul T, Vanisri H, et al., 2006. Rainbow refractrometry: on the validity domain of Airy's and Nussenzveig's theories. *Optics Communications*, 259(1):7-13. https://doi.org/10.1016/j.optcom.2005.08.031

Saengkaew S, Charinpanitkul T, Vanisri H, et al., 2007. Rainbow refractrometry on particles with radial refractive

index gradients. *Experiments in Fluids*, 43(4):595-601. https://doi.org/10.1007/s00348-007-0342-y

Saengkaew S, Godard G, Blaisot J, et al., 2009. Experimental analysis of global rainbow technique: sensitivity of temperature and size distribution measurements to non-spherical droplets. *Experiments in Fluids*, 47:839-848. https://doi.org/10.1007/s00348-009-0680-z

Song F, Xu C, Wang S, et al., 2016. Measurement of temperature gradient in a heated liquid cylinder using rainbow refractometry assisted with infrared thermometry. *Optics Communications*, 380:179-185. https://doi.org/10.1016/j.optcom.2016.06.011

van Beeck J, Riethmuller M, 1996. Rainbow phenomena applied to the measurement of droplet size and velocity and to the detection of nonsphericity. *Applied Optics*, 35(13):2259-2266. https://doi.org/10.1364/AO.35.002259

van Beeck J, Giannoulis D, Zimmer L, et al., 1999. Global rainbow thermometry for droplet-temperature measurement. *Optics Letters*, 24(23):1696-1698. https://doi.org/10.1364/OL.24.001696

Verdier A, Santiago JM, Vandel A, et al., 2016. Experimental study of local flame structures and fuel droplet properties of a spray jet flame. *Proceedings of the Combustion Institute*, 36(2):2595-2602. https://doi.org/10.1016/j.proci.2016.07.016

Whitaker S, 1972. Forced convection heat transfer correlations for flow in pipes, past flat plates, single cylinders, single spheres, and for flow in packed beds and tube bundles. *AIChE Journal*, 18(2):361-371. https://doi.org/10.1002/aic.690180219

Wilms J, Weigand B, 2007. Composition measurements of binary mixture droplets by rainbow refractometry. *Applied Optics*, 46(11):2109-2118. https://doi.org/10.1364/AO.46.002109

Wu X, Wu Y, Saengkaew S, et al., 2012. Concentration and composition measurement of sprays with a global rainbow technique. *Measurement Science and Technology*, 23(12): 125302. https://doi.org/10.1088/0957-0233/23/12/125302

Wu X, Jiang H, Wu Y, et al., 2014. One-dimensional rainbow thermometry system by using slit apertures. *Optics Letters*, 39(3):638-641. https://doi.org/10.1364/OL.39.000638

Wu X, Li C, Jiang H, et al., 2017. Measurement error of global rainbow technique: the effect of recording parameters. *Optics Communications*, 402:311-318. https://doi.org/10.1016/j.optcom.2017.06.018

Yu H, Xu F, Tropea C, 2013a. Optical caustics associated with the primary rainbow of oblate droplets: simulation and application in non-sphericity measurement. *Optics Express*, 21(22):25761-25771. https://doi.org/10.1364/OE.21.025761

Yu H, Xu F, Tropea C, 2013b. Simulation of optical caustics associated with the secondary rainbow of oblate droplets. *Optics Letters*, 38(21):4469-4472. https://doi.org/10.1364/OL.38.004469

Zhao Y, Qiu H, 2006. Measurements of multicomponent microdroplet evaporation by using rainbow refractometer and PDA. *Experiments in Fluids*, 40(1):60-69. https://doi.org/10.1007/s00348-005-0046-0

Zumdahl, SS, 2009. Chemical Principles. Houghton Mifflin Company, Boston, USA.

中文概要

题　目：彩虹折射法对喷雾气液沉淀反应的原位表征

目　的：喷雾气液吸收化学反应广泛存在于能源、化学和环境工程中。比如在能源环境领域，湿法烟气脱硫（WFGD）中的碱性喷雾吸收脱除气体污染物，乙醇胺（MEA）吸收脱除 CO_2 酸性气体。对这类反应的表征，有利于控制和改善污染物脱除效率。本文尝试利用气液吸收沉淀反应过程中液滴折射率的变化来原位表征反应进程。

创新点：1. 基于彩虹折射法，首次对气液吸收沉淀反应的原位表征进行探究；2. 通过若干实验和详细的传热计算分析，成功验证了其可行性和有效性。

方　法：1. 通过与 Abbe 折射仪对比，确定全场彩虹测量的准确性（图 3 和公式（5））；2. 搭建全局彩虹技术（GRT）测量系统进行喷雾测量实验（图 2），并记录反应过程中的彩虹图像和离线采样液滴用于显微分析（图 4 和 5）；3. 对涉及到的气液吸收沉淀反应进行传热计算和分析（公式（7）~（13））。

结　论：1. 初步表明了利用溶液折射率表征 $Ca(OH)_2$ 质量分数的可行性。2. 实验结果表明 GRT 的测量结果精确；反应后液滴折射率减少并趋向于水，反应进程可体现在彩虹角（即折射率）的变化上。3. 不同浓度 $Ba(OH)_2$ 吸收 CO_2 的反应进一步证明了该方法原位表征气液吸收沉淀反应的可行性。4. 反应的传热计算和分析表明反应热所造成的温度升高可以忽略，验证了该方法的有效性。

关键词：彩虹折射法；原位表征；折射率；气液吸收沉淀反应